

# Reliability-guided digital image correlation for image deformation measurement

Bing Pan

School of Mechanical and Aerospace Engineering, Nanyang Technological University,  
50, Nanyang Avenue, Singapore 639798

\*Corresponding author: panb04@mails.tsinghua.edu.cn

Received 5 January 2009; revised 9 February 2009; accepted 9 February 2009;  
posted 10 February 2009 (Doc. ID 105971); published 4 March 2009

A universally applicable reliability-guided digital image correlation (DIC) method is proposed for reliable image deformation measurement. The zero-mean normalized cross correlation (ZNCC) coefficient is used to identify the reliability of the point computed. The correlation calculation begins with a seed point and is then guided by the ZNCC coefficient. That means the neighbors of the point with the highest ZNCC coefficient in a queue for computed points will be processed first. Thus the calculation path is always along the most reliable direction, and possible error propagation of the conventional DIC method can be avoided. The proposed novel DIC method is universally applicable to the images with shadows, discontinuous areas, and deformation discontinuity. Two image pairs were used to evaluate the performance of the proposed technique, and the successful results clearly demonstrate its robustness and effectiveness. © 2009 Optical Society of America

*OCIS codes:* 100.2000, 120.3940, 120.6150, 120.6650.

## 1. Introduction

Two-dimensional (2D) digital image correlation (DIC) [1–5], three-dimensional (3D) DIC [1,6], and the shadow speckle method (or speckle projection profilometry) [7] have been extensively investigated and widely used for in-plane deformation (2D DIC), 3D shape and deformation (3D DIC), as well as 3D shape and out-of-plane displacement (shadow speckle method) measurements. While using these correlation-based techniques, the most important task is to reliably and accurately measure the motion of each image point (i.e., image deformation), which is normally carried out by matching or tracking the same image points located in the two images recorded in different states or by different cameras from different orientations. Only when the image deformation is accurately determined can it be further converted to the desired physical quantities, such as displacement of the test object surface and height information of each point.

Before the implementation of DIC analysis, a region of interest (ROI) should be specified or defined in the reference image. The regularly spaced points within the ROI are considered as valid points to be computed. The conventional correlation calculation generally starts with the upper left point of the ROI. Then the calculation analysis is carried out point by point along each row or column. To accurately determine the displacement components, subpixel displacement using the Newton–Raphson (NR) method is highly recommended [2]. Because the NR method is able to take the deformation of the subset into consideration, it is unaffected by large strains and/or rotations of the deformed image [8–10]. While using the NR method, the initial guess is quite important, because it directly affects the converge characteristics of the algorithm [9]. Normally, to speed calculation and save computation time, the computed displacements and strains of the current point are used as the initial guess of the next point according to the continuous deformation assumption. In this sense the conventional pointwise DIC computation is a path-dependent approach. Although we can estimate the initial guess separately for each point, this

approach is either impractical because it is extremely time-consuming or impossible if large deformation or rotation is present in the deformed image.

So even though the well-established conventional DIC method is effective in most cases, this path-dependent approach may give rise to wrong results in the following cases. First, if the digital images of the practical test object contain discontinuous areas such as cracks, holes, or other discontinuous area, or if an irregular ROI is defined in the reference image, the transfer of initial guess will fail to provide reliable initial guess for the next point in some locations. Second, if apparent discontinuous deformation occurs in the deformed image, the transfer of initial guess also fails. Third, an occasionally occurring faulty data point will also provide a wrong initial guess for the next point. In all these cases, if one point is wrongly computed, the results of bad points will be passed to the next point, leading to the propagation of error. It should be noted that the so-called continuum (or global) DIC method based on B-spline function proposed by Cheng *et al.* [11] or the finite element formulation proposed by Sun *et al.* [12] may be able to cope with these problems to some extent by ensuring the displacement continuity and displacement gradients continuity among calculation points; however, the implementation of the continuum DIC method is very complicated and computation intensive.

Here a novel and universally applicable reliability-guided digital image correlation (RGDIC) method is proposed to overcome the disadvantage of the conventional DIC method. The central idea of the proposed technique is that the deformation parameters of the computed point with highest zero-mean normalized cross correlation (ZNCC) coefficient [4] in a queue for computed points are used as the initial guess of its neighboring points to continue correlation analysis. This means the neighbors of the point with highest ZNCC coefficient will be computed earlier. It is necessary to note that a similar concept has been used in a reliability-guided phase unwrapping algorithm [13–15] in fringe pattern analysis. However, in a reliability-guided phase unwrapping

algorithm, the reliability parameter map is built before computation. According to this map the reliability-guided phase unwrapping algorithm unwraps the pixels with highest reliability. Thus, if there is any error, it is limited to local minimum areas [13]. In contrast, the RGDIC method is quite different from the reliability-guided phase unwrapping algorithm in that we can not generate a reliability parameter map to guide the computation path before correlation analysis. In the RGDIC method the correlation calculation begins with a seed point and is then guided by ZNCC coefficients of the computed points. This ensures the calculation path is always along the most reliable direction and error propagation is avoided. Thus the proposed algorithm is insensitive to the discontinuous area and deformation contained in the deformed image. It is universally applicable to the deformation measurement of the images with any deformation state. To verify the performance of the proposed method, two image pairs acquired from 3D DIC and shadow speckle experiments are employed in validation experiments. Experimental results clearly demonstrate the robustness and effectiveness of the novel method.

## 2. Reliability-Guided Digital Image Correlation

### A. Basic Principle of Digital Image Correlation

In essence DIC is a deformation measurement technique based on digital image processing and numerical computing. The basic principle of DIC is schematically illustrated in Fig. 1. A square reference subset of  $(2M + 1) \times (2M + 1)$  pixels centered at the current point  $P(x_0, y_0)$  from the reference image is chosen and used to find its corresponding location in the target image. Once the location of the target subset in the deformed image is found, the displacement components of the reference and target subset centers can be determined. In practical implementation of DIC, a ROI in reference image must be specified first and further divided into evenly spaced virtual grids. The displacements are computed at each point of the virtual grids to obtain the full-field deformation.

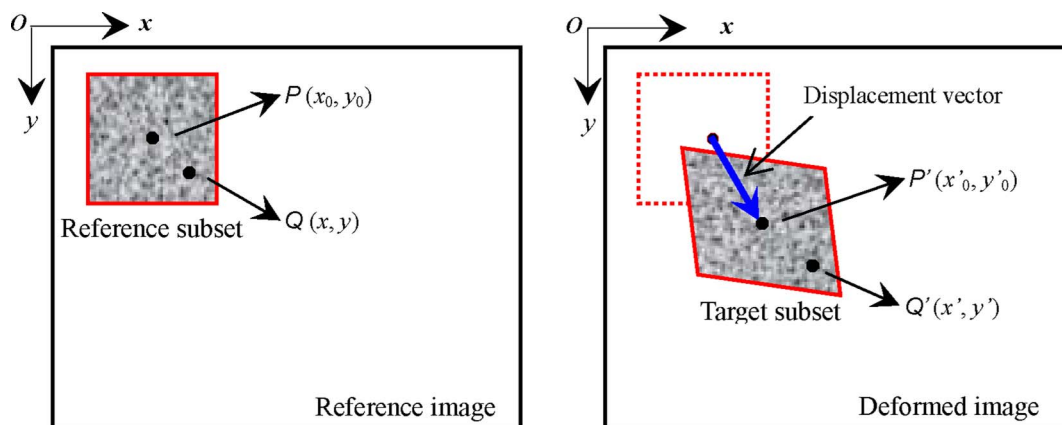


Fig. 1. (Color online) Basic principle of the DIC method.

To obtain accurate estimation for the displacement components of the same point in the reference and target images, the following zero-normalized sum of squared differences (ZNSSD) correlation criteria [4], which is insensitive to the scale and offset of illumination lighting fluctuations, is utilized to evaluate the similarity of reference and target subsets:

$$C_{\text{ZNSSD}}(\mathbf{p}) = \sum_{x=-M}^M \sum_{y=-M}^M \left[ \frac{f(x,y) - f_m}{\sqrt{\sum_{x=-M}^M \sum_{y=-M}^M [f(x,y) - f_m]^2}} - \frac{g(x',y') - g_m}{\sqrt{\sum_{x=-M}^M \sum_{y=-M}^M [g(x',y') - g_m]^2}} \right]^2, \quad (1)$$

where  $f(x,y)$  is the gray level intensity at coordinates  $(x,y)$  in the reference subset of the reference image,

$$\begin{aligned} x' &= x_0 + \Delta x + u + u_x \Delta x + u_y \Delta y + \frac{1}{2} u_{xx} \Delta x^2 + \frac{1}{2} u_{yy} \Delta y^2 + u_{xy} \Delta x \Delta y, \\ y' &= y_0 + \Delta y + v + v_x \Delta x + v_y \Delta y + \frac{1}{2} v_{xx} \Delta x^2 + \frac{1}{2} v_{yy} \Delta y^2 + v_{xy} \Delta x \Delta y. \end{aligned} \quad (4)$$

$g(x',y')$  is the gray level intensity at coordinates  $(x',y')$  in the target subsets of the deformed image,

$$f_m = \frac{1}{(2M+1)^2} \sum_{x=-M}^M \sum_{y=-M}^M [f(x,y)],$$

$$g_m = \frac{1}{(2M+1)^2} \sum_{x=-M}^M \sum_{y=-M}^M [g(x',y')],$$

are the mean intensity values of reference and target subsets, respectively, and  $\mathbf{p}$  denotes the desired vector with respect to displacement mapping function used.

It is necessary to point out that the ZNSSD correlation criterion is actually related to the commonly used ZNCC according to the following equation [4]:

$$C_{\text{ZNCC}}(\mathbf{p}) = \frac{\sum_{x=-M}^M \sum_{y=-M}^M [f(x,y) - f_m] \times [g(x',y') - g_m]}{\sqrt{\sum_{x=-M}^M \sum_{y=-M}^M [f(x,y) - f_m]^2} \sqrt{\sum_{x=-M}^M \sum_{y=-M}^M [g(x',y') - g_m]^2}} = 1 - 0.5 \times C_{\text{ZNSSD}}(\mathbf{p}). \quad (2)$$

Because of its simplicity, in this work the ZNSSD correlation criterion is optimized using the NR method for computing displacement components of each calculation point. But the computed ZNSSD coefficient is then converted to the ZNCC coefficient according to Eq. (2) and is used as reliability to guide the

correlation calculation in the proposed RGDIC method, because the ZNCC coefficient with a range of  $[-1,1]$  is quite intuitive to show the similarity between the reference subset and target subset.

In Eq. (1) the point  $(x,y)$  in the reference subset can be mapped to the point  $(x',y')$  in the target subset according to the so-called “displacement mapping function” [10]. The commonly used first-order displacement mapping function [8] is given as

$$\begin{aligned} x' &= x_0 + \Delta x + u + u_x \Delta x + u_y \Delta y, \\ y' &= y_0 + \Delta y + v + v_x \Delta x + v_y \Delta y. \end{aligned} \quad (3)$$

The second-order displacement mapping function [6,7,10], which is capable of approximating more complicated deformation of the deformed subset, is expressed as

In Eqs. (3) and (4),  $u$  and  $v$  are the displacement components for the subset center in the  $x$  and  $y$  directions, respectively;  $\Delta x = x - x_0$  and  $\Delta y = y - y_0$  are the distances from the subset center  $(x_0, y_0)$  to point  $(x, y)$ ;  $u_x, u_y, v_x,$  and  $v_y$  are the displacement gradient components; and  $u_{xx}, u_{yy}, u_{xy}, v_{xx}, v_{yy},$  and  $v_{xy}$  are the second-order displacement gradient components of the subset.

It is evident that Eq. (1) is the nonlinear function of 6 or 12 unknown parameters, depending on the displacement mapping function used. Equation (1) can be optimized to get the desired in-plane displacement components in the  $x$  and  $y$  directions using the following classic NR iteration method [4]:

$$\mathbf{p} = \mathbf{p}_0 - \frac{\nabla C(\mathbf{p}_0)}{\nabla \nabla C(\mathbf{p}_0)}, \quad (5)$$

where  $\mathbf{p}_0$  is the initial guess of the solution, which can be achieved through a simple integer pixel dis-

placement searching process or other approach [16],  $\mathbf{p}$  is the next iterative approximation solution of Eq. (5),  $\nabla C(\mathbf{p}_0)$  is the gradients of correlation criteria, and  $\nabla \nabla C(\mathbf{p}_0)$  are the second-order derivatives of correlation criteria, commonly called Hessian matrix, which can be further approximated to simplify

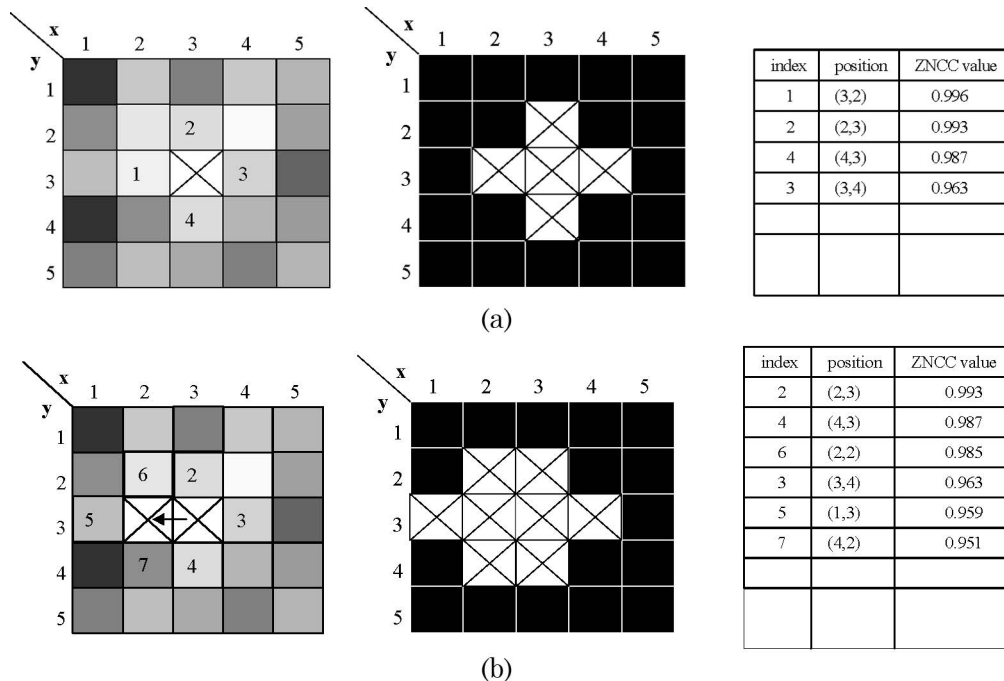


Fig. 2. Example of RGDIC based on the computed ZNCC coefficient value.

calculation without loss of accuracy [9]. A detailed description of the NR method with ZNCC criterion can be found in [4].

#### B. Reliability-Guided Digital Image Correlation

In the conventional DIC method, if some points are wrongly computed due to area discontinuity and/or deformation discontinuity and/or other reasons, the results of bad points will be transferred to the next point, leading to the propagation of error. Here the so-called RGDIC method using the ZNCC coefficient as reliability parameter is proposed to cope with the problem.

Similar to the approach used in reliability-guided phase unwrapping [13], in the practical implementation of the proposed RGDIC method, a queue  $Q$  and two binary masks  $M_v$  and  $M_c$  with the same size of digital image should be built. If a point has been computed, it is subsequently inserted into the queue  $Q$  according to the magnitude of its correlation coefficient. The binary mask  $M_v$  is to identify the valid points to be computed or not to be computed. It can be defined after the ROI and grid step is specified in the reference image. In mask  $M_v$ , valid points to be computed are set as 1 otherwise 0. The other binary mask  $M_c$  denotes the valid points have been computed. The initial value of each pixel in  $M_c$  is set to 0. If one point has been computed, its corresponding position in mask  $M_c$  is set to 1. Besides, it is quite important to mention that a good seed point (or starting point) that can be accurately and reliably searched in the deformed image must be specified first. The deformation and ZNCC correlation coefficient of the seed point can be computed using automatic searching scheme or other techniques [16].

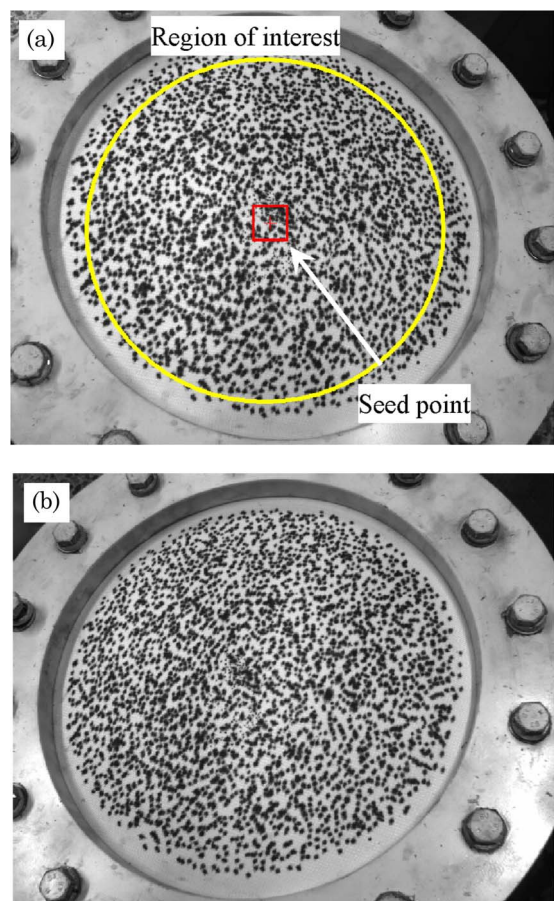


Fig. 3. (Color online) (a) Left image and (b) right image of the composite film surface. The yellow ellipse of the reference image is the defined ROI, and the inner red square shows the selected seed point and its subset.

A detailed description of the proposed RGDIC method is as follows:

1. The four neighboring points of the seed point are computed. Then these computed points are marked as 1 in the binary mask  $M_c$ . Afterward the four neighboring points are inserted into the queue  $Q$  according to their ZNCC correlation coefficients from higher to lower one. Figure 2(a) shows an example of a  $5 \times 5$  points local area.

2. The first point with maximum ZNCC correlation coefficient is removed from the top of the queue. Then each of its four neighboring points is judged as to whether it is a valid point to be computed and has not been computed. If it is a valid point (i.e.,  $M_v = 1$ ) and not computed (i.e.,  $M_c = 0$ ), then its displacements and strains are computed using the NR method. Note that the computed deformation parameters of the removed points are used as initial guess for its neighbors. Subsequently, these calculated points are labeled as one in the binary mask  $M_c$  and inserted into the queue according to its ZNCC correlation coefficient order, as shown in Fig. 2(b).

3. Step 2 is repeated until the queue is empty, which means that all points have been computed

and the correlation computation is finished.

From this description it is evident that the correlation analysis is always performed along the points with highest ZNCC coefficient in the queue. If some points are wrongly computed with low ZNCC coefficient, the computation of its neighbors will be postponed. Thus the proposed algorithm is insensitive to the discontinuous area and deformation contained in the deformed image and is universally applicable to the deformation measurement of the image with discontinuities.

### 3. Experimental Verification

Here two image pairs taken from previous experiments will be processed to verify the performance of the RGDIC method. In the following calculation the NR algorithm with second-order displacement mapping function is employed to optimize the ZNCC criterion to get the desired deformation parameters for each point, and the subset used is  $41 \times 41$  pixels and the grid step (i.e., the distance between neighboring points) is set as 5 pixels.

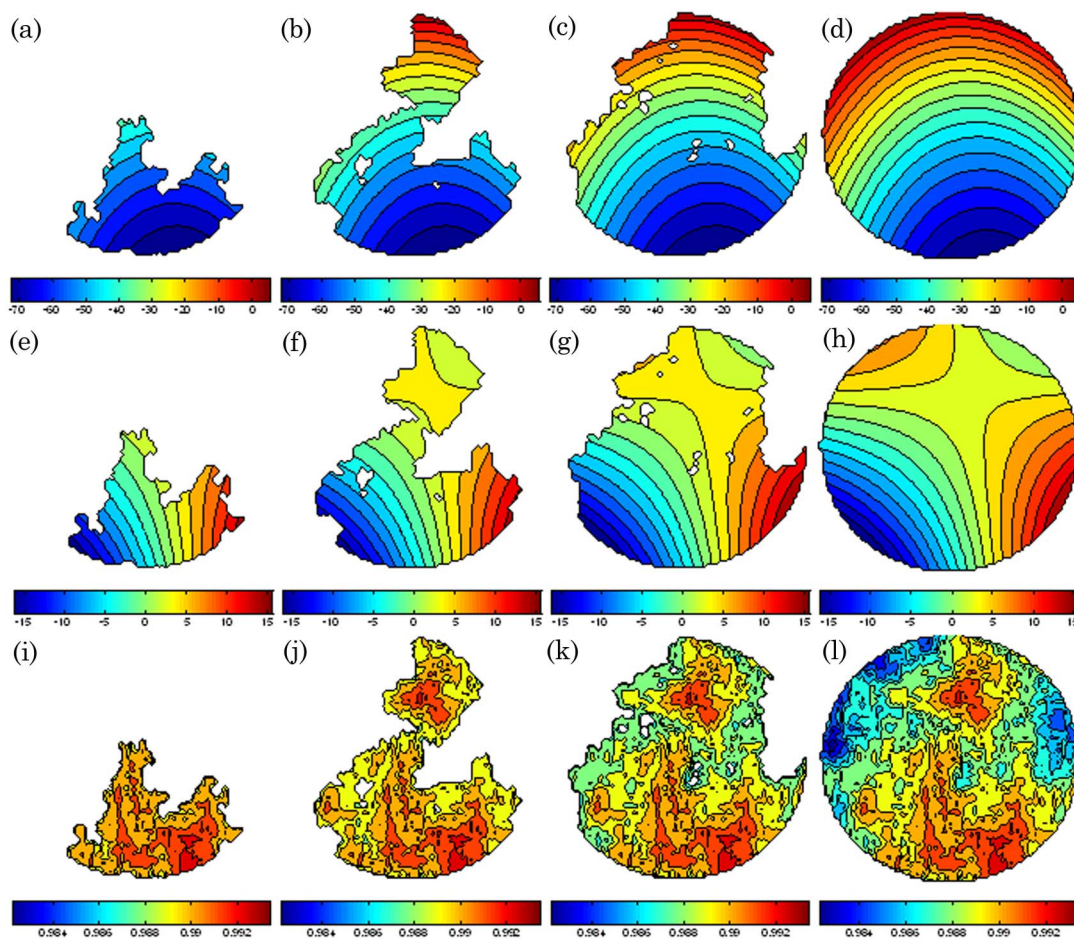


Fig. 4. (Color online) Three intermediate stages and the final results of the computed  $u$  displacement (top),  $v$  displacement (middle), and ZNCC coefficient (bottom) distributions using the RGDIC method.

### A. Stereo Image Pair of the Three-Dimensional Digital Image Correlation Experiment

The first test image pair, as shown in Fig. 3, was taken from the 3D DIC experiment. The 3D DIC based on a combination of the binocular stereo vision and DIC technique can be used for 3D shape and deformation measurement of curved surface. In the 3D DIC technique, stereo vision calibration and stereo matching of homograph points are two crucial steps [17]. The task of stereo matching is to precisely match the same physical point recorded in the left and right images, which is commonly considered as the most difficult part in stereo vision.

In the experiment the speckle images of a multilayer composite film was recorded using two cameras from different orientations. The purpose of the experiment is to reconstruct the 3D profile and determine the 3D deformation of the test multilayer composite film surface caused by various inner pressures in a bugle test. The two images shown in Fig. 3 were recorded with an inner water pressure of 0.4 kPa.

Because only the deformation of the film surface is concerned, an irregular ROI is defined as indicated in Fig. 3(a). For the calculation points within an irregular ROI, conventional DIC method is prone to provide the wrong results in some locations. Using the proposed RGDIC method, the calculation starts from the seed point and is then guided by the ZNCC coefficient of computed points. The computed  $u$  displacement and  $v$  displacement fields using the RGDIC method are shown in Figs. 4(d) and 4(h), respectively. In Fig. 4(i) the computed ZNCC coefficients are all larger than 0.98, which proves the reliability of the computation. Figure 4 also gives the intermediate stages of the computed  $u$  displacement,  $v$  displacement, and ZNCC coefficient distributions using the RGDIC method. From the four stages of the ZNCC coefficient distributions, we can clearly see that the displacements were computed from the points with a larger ZNCC coefficient to the points with a small ZNCC coefficient. For example, the points located

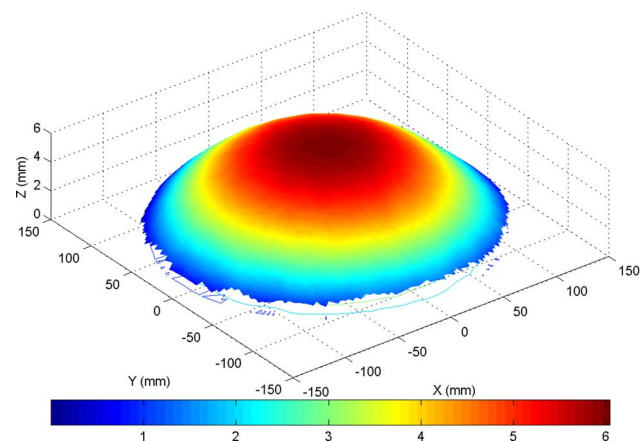


Fig. 5. (Color online) Reconstructed 3D shape of the composite film surface subjected to 0.4 kPa inner pressure.

in the upper left and upper right areas of the ROI are computed later since the ZNCC coefficients of these points are smaller than those of other points, as can be seen from Fig. 4.

In the experiment the stereo vision calibration technique used in [6] was employed to calibrate the intrinsic parameters (i.e., effective focal length, principal point, and lens distortion coefficient) and extrinsic parameters (i.e., the 3D positions and orientations of the camera relative to a world coordinate system) of each camera. Based on these calibrated parameters and computed disparity data using the RGDIC method, we can reconstruct the 3D shape of the composite film surface as illustrated in Fig. 5. The 3D profile of the film due to inner pressure is in accordance with practical situation.

### B. Image Pair of Shadow Speckle Experiment

The second test image pair as shown in Fig. 6 was acquired in a shadow speckle experiment. The shadow speckle method combines the projection of

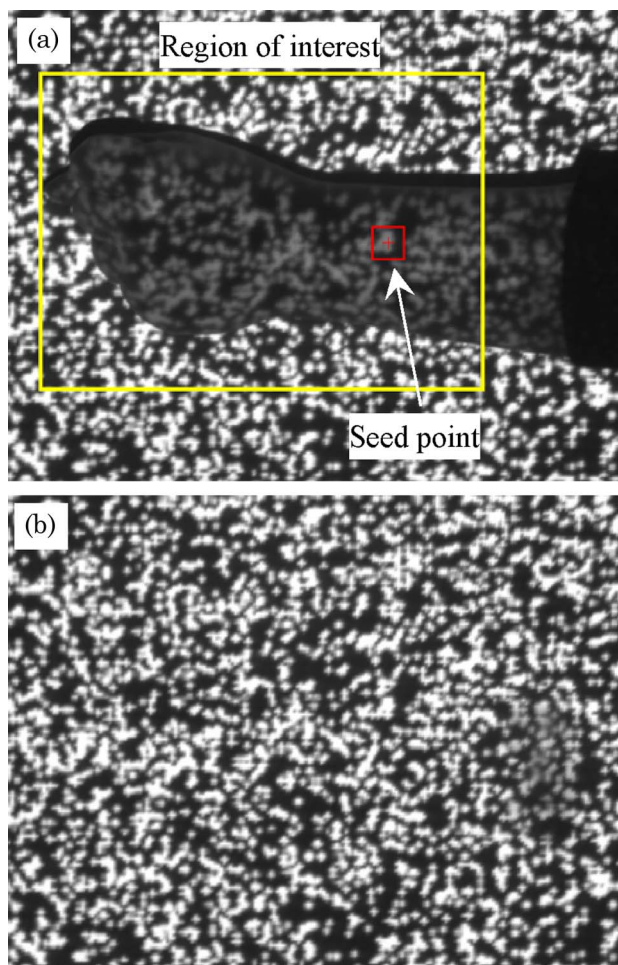


Fig. 6. (Color online) (a) Reference image and (b) target image. The yellow rectangle of the reference image is the defined ROI, and the inner red square illustrates the selected seed point and its subset.

computer-generated random speckle pattern onto the reference plane using an ordinary LCD projector and the 2D DIC for in-plane displacements measurement [7]. The computer-generated speckle pattern is projected onto the reference plane first and then projected onto the test object surface placed onto the reference plane. The out-of-plane height of the specimen surface results in the in-plane motion of the projected speckle pattern. By detecting the in-plane displacements of the projected speckle pattern, the height of the test specimen surface relative to the reference plane can be restored. Figure 6 shows the speckle pattern projected onto a human hand and the reference plane. It is clearly seen from Fig. 6(a) that shadows exist due to the shading of the hand. The specified ROI is plotted as a yellow rectangle in Fig. 6(a).

Figure 7 shows the two intermediate stages, and the final results of the computed  $v$  displacement field (the computed  $u$  displacement is quite small and not given in the following) and ZNCC coefficient distribution. Although serious decorrelation effect exists in the boundary of the hand due to steep height change and shadows, the whole  $v$  displacement field is also reliably and accurately determined as shown in

Fig. 7(e). Owing to the decorrelation effect, these points located in the boundary of the hand are incorrectly computed with lower ZNCC coefficient; however, we can clearly see from Fig. 7 that these points are processed later. As a result of this procedure, the errors of these points are limited to local minimum areas and bring no influence to other points.

In contrast with the ZNCC coefficient distribution given in Fig. 7(f), it is evident that the computed displacements of points with low correlation coefficient are also unreliable. Thus, according to the ZNCC coefficient distribution, we can select a threshold of ZNCC coefficient (i.e., 0.8) to remove the unreliably computed points. Based on the calibrated displacement-to-height relation [7] and the  $v$  displacement components, the profile of the human hand can be reconstructed as shown in Fig. 8. Figure 8(a) shows the contour plot of the measured hand profile superimposed on the image of the hand. Figure 8(b) gives a 3D plot of the hand profile, which provides a more intuitive look. The reconstructed profile clearly shows the flexibility and robustness of the proposed RGDIC method.

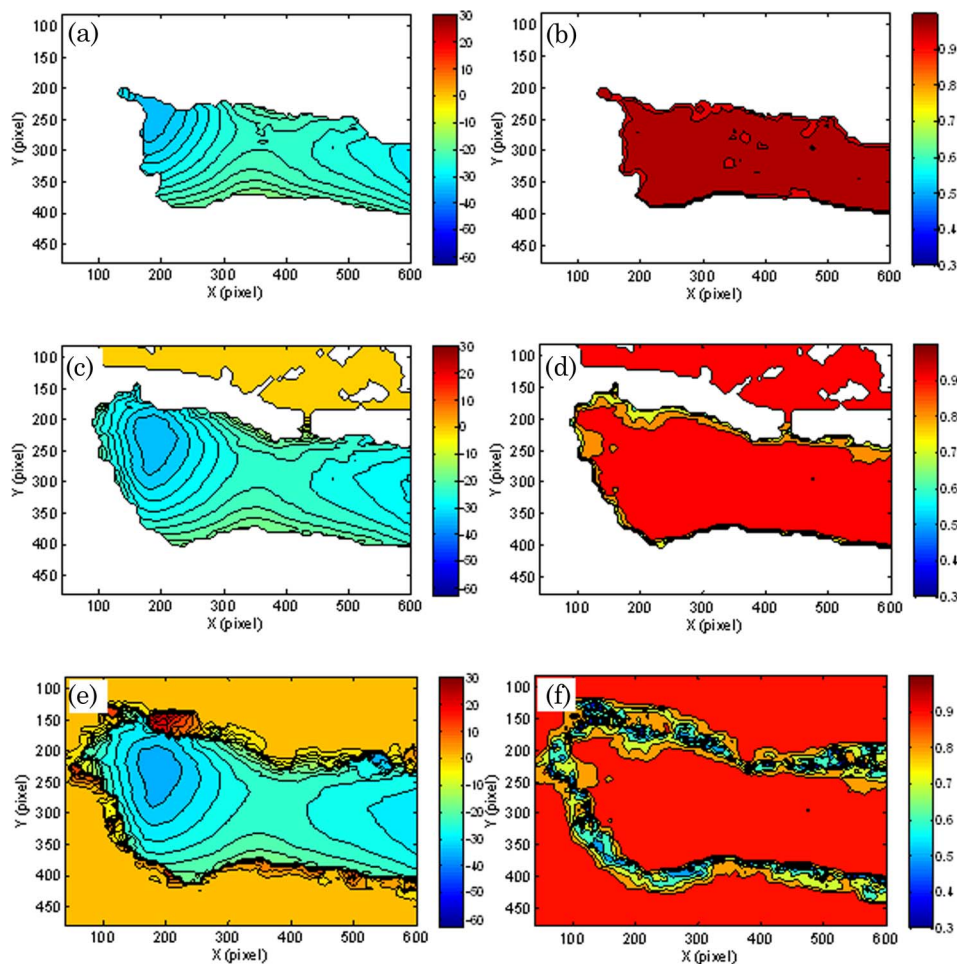


Fig. 7. (Color online) Intermediate stages of the computed  $v$  displacement (left) and ZNCC coefficient (right) distributions using the RGDIC method. It is clear that serious decorrelation effect exist at the boundary of the hand.

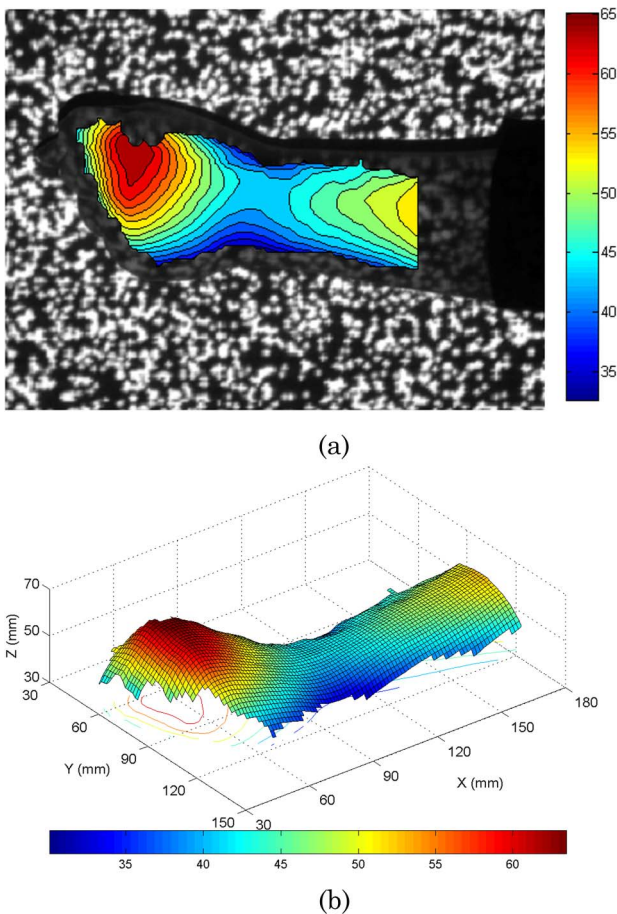


Fig. 8. (Color online) Reconstructed profile of a human hand after threshold using ZNCC coefficient distribution: (a) contour plot and (b) 3D plot.

#### 4. Conclusion

The RGDIC method is proposed for reliable and accurate image deformation measurement. The correlation analysis begins with a selected seed point and proceeds with neighbors around the point with highest ZNCC. Thus the calculation path is always along the most reliable direction, and possible error propagation is avoided. The proposed RGDIC method is very robust and effective. It is universally applicable to experimental images with shadows, discontinuous areas, and deformation discontinuity. The image deformation of two pairs of speckle image acquired in 3D DIC and speckle projection profilometry experiments were correctly computed, which clearly indicates the robustness and validity of the proposed reliability-guided DIC method.

I express my sincere gratitude to X. Huimin of Tsinghua University and A. Asundi of Nanyang

Technological University for their encouragement and support.

#### References

1. M. A. Sutton, S. R. McNeill, J. D. Helm, and Y. J. Chao, "Advances in two-dimensional and three-dimensional computer vision," P. K. Rastogi, ed., *Topics in Applied Physics* (Springer Verlag, 2000), Vol. 77, pp. 323–372.
2. B. Pan, H. M. Xie, B. Q. Xu, and F. L. Dai, "Performance of sub-pixel registration algorithms in digital image correlation," *Meas. Sci. Technol.* **17**, 1615–1621 (2006).
3. B. Pan, H. M. Xie, Z. Y. Wang, and K. M. Qian, "Study of subset size selection in digital image correlation for speckle patterns," *Opt. Express* **16**, 7037–7048 (2008).
4. B. Pan, H. M. Xie, Z. Q. Guo, and T. Hua, "Full-field strain measurement using a two-dimensional Savitzky–Golay digital differentiator in digital image correlation," *Opt. Eng.* **46**, 033601 (2007).
5. B. Pan, A. Asundi, H. M. Xie, and J. X. Gao, "Digital image correlation using iterative least squares and pointwise least squares for displacement field and strain field measurements," *Opt. Lasers Eng.* (to be published).
6. B. Pan, H. M. Xie, L. H. Yang, and Z. Y. Wang, "Accurate measurement of satellite antenna surface using three-dimensional digital image correlation technique," *Strain* (to be published).
7. B. Pan, H. Xie, J. Gao, and A. Asundi, "Improved speckle projection profilometry for out-of-plane shape measurement," *Appl. Opt.* **47**, 5527–5533 (2008).
8. H. A. Bruck, S. R. McNeil, M. A. Sutton, and W. H. Peters, "Digital image correlation using Newton–Raphson method of partial differential correction," *Exp. Mech.* **29**, 261–267 (1989).
9. G. Vendroux and W. G. Knauss, "Submicron deformation field measurements. Part 2. Improved digital image correlation," *Exp. Mech.* **38**, 86–92 (1998).
10. H. Lu and P. D. Cary, "Deformation measurement by digital image correlation: implementation of a second-order displacement gradient," *Exp. Mech.* **40**, 393–400 (2000).
11. P. Cheng, M. A. Sutton, H. W. Schreier, and S. R. McNeill, "Full-field speckle pattern image correlation with B-spline deformation function," *Exp. Mech.* **42**, 344–352 (2002).
12. Y. Sun, J. H. L. Pang, C. K. Wong, and F. Su, "Finite element formulation for a digital image correlation method," *Appl. Opt.* **44**, 7357–7363 (2005).
13. X. Su and W. Chen, "Reliability-guided phase unwrapping algorithm: a review," *Opt. Lasers Eng.* **42**, 245–261 (2004).
14. S. Li, W. Chen, and X. Su, "Reliability-guided phase unwrapping in wavelet-transform profilometry," *Appl. Opt.* **47**, 3369–3377 (2008).
15. Q. Kemao, W. Gao, and H. Wang, "Windowed Fourier-filtered and quality-guided phase-unwrapping algorithm," *Appl. Opt.* **47**, 5420–5428 (2008).
16. B. Pan, H. M. Xie, Y. Xia, and Q. Wang, "Large deformation measurement based on reliable initial guess in digital image correlation method," *Acta Optica Sinica* (in Chinese) (to be published).
17. D. Garcia, J. J. Orteu, and L. Penazzi, "A combined temporal tracking and stereo-correlation technique for accurate measurement of 3D displacements: application to sheet metal forming," *J. Mater. Process. Technol.* **125**, 736–742 (2002).